

SYNTHESIS INVESTIGATION FOR A MAGNETIC PROJECTOR LENS**Tareq Hashim Abbood, Saadi R. Abbas and Muhssen Salbookh Erhayief**

Department of Physics, College of Education, Mustansiriyah University, and P.O. Box: 46219, Baghdad, Iraq.

ABSTRACT

A computational investigation has been carried out to investigate the inverse design problem for a magnetic projector lenses. Actually, an analytical expression has proposed to approximate the magnetic scalar potential. Indeed, this target function has a simple mathematical representation and involves three-optimization parameters. With aid of the proposed target function, the corresponding magnetic field has deduced analytically. Thereafter, the paraxial-ray equation solved by means of fourth order Runge-Kutta method to deduce the electron beam trajectory along the lens interval. Ultimately, the radial and spiral distortion evaluated and optimized in terms of the proposed optimization parameters. Results have shown an impressive remark that, the optimum lens could be operated at a certain excitation parameter where the radial and spiral almost vanishes at the first magnification point approximately.

Keywords: Electron and Ion optics, Magnetic Lenses, Projector properties, Electron microscope, Distortion.

1. INTRODUCTION

It is well-known that due to the electric charge that electrons have they can be deflected by means of electric and/or magnetic fields. The instrument that performs such a function called lens or precisely electron lens. Magnetic lens is one of the most important sorts of electron lenses where modern electron microscopes (EM) are equipped with them. These lenses usually produce magnetic fields in a narrow circular gap between two pole pieces. The amount of deduced field is typically of order of 1.0 Tesla [1]. Magnetic lens named condenser, objective and projector according to its own role throughout the electron microscope column specifically the transmission one. The main task of projector lens is to be magnifying the final image produced by the objective lens.

Unfortunately, projector lens suffers from several defects that leads to distorting the magnified image without affecting the resolution [2]. In addition to the image rotation, the radial and spiral distortions are the most important defects that inherent with the work of projector lens. Indeed, the first significant attempt to eliminate radial distortion had presented by Hillier in 1946, where this endeavor based theoretically and experimentally [3]. Actually, this investigation had opened a new horizon to vanishing image rotation that explored by many authors [4,5 and 6]. Concerning with distortions defects, several efforts have introduced to eliminate or at least reduce these defects concerning the experimental point of view [7 and 8]. However, as long as the computational investigation is concerned one may argue many literatures, see for example [9, 8, 10, 11 and 12].

Present work put forward to investigates radial and spiral distortion for a synthesized magnetic lens. Indeed, such a lens needs to inversely be reconstructed in terms of analytical formula that representing the magnetic scalar potential. Anyway, this formula should treat to be a target function characterized by three-optimization parameters. Therefore, the behavior of both of the two-regarded distortion can be outlined [19][20].

2. METHOD

The target function adopted in the this work is formulated by the following expression [13];

$$V(z) = \frac{1}{2} \left[(V_1 + V_2) + (V_2 - V_1) \tanh\left(\frac{1.32z}{R}\right) \right] \quad (1)$$

Magnetic lens's (magnetic scalar potential distribution $V(z)$). Where R is the radius of the pole piece and V_1 and V_2 are potential values at the proposed lens' terminals, i.e., $V_1=V_s$ and $V_2=V_f$. The axial component of the magnetic field may be calculated using the equation $[B_z = -\mu_0 \text{grad}V]$ as follows:

$$B_z(z) = -\mu_0 \frac{dV(z)}{dz} \quad (2)$$

μ_0 : magnetic permeability in a vacuum is where ($4\pi \times 10^{-7} \text{ Hm}^{-1}$). Hence, the substitution of eq. (1) in equation (2) leads to deduce the axial magnetic field distribution to be as follows;

$$B_z(z) = \mu_0 \left(\frac{V_2 - V_1}{2} \right) \left(\frac{1.32z}{R} \right) \text{sech}^2 \left(\frac{1.32z}{R} \right) \quad (3)$$

With aid of equation (3) the dispersion of the imaging magnetic field It is possible to assign $B_z(z)$ along the optical axis $z_s \leq z \leq z_f$. The calculation of the electron beam trajectory $r(z)$ and its corresponding departure $r'(z)$ along the axis of the lens must be done once a magnetic field has been identified. The paraxial ray equation supplied may often be solved to complete this assignment by the relation [14];

$$r'' + \frac{\eta}{8V_r} B_z^2(z)r = 0 \quad (4)$$

where η is the ratio of an electron's mass (m) to charge (e), and V_r is the relativistically corrected accelerating voltage, which is determined by [15];

$$V_r = V_a \left(1 + \frac{eV_a}{2mc^2} \right) = V_a (1 + 0.978 \times 10^{-6} V_a) \quad (5)$$

The symbol V_a refers to the voltage used to accelerate. It is well known that the optical qualities of magnetic lenses depend on the charge to mass ratio of the charged particles utilized [16] as their distinguishing feature. The paraxial ray equation (4) must be solved in accordance with the limitations placed on the problem in order to get the electron beam trajectory within the electron lens. However, this problem has been numerically solved using infinite magnification mode and the fourth-order Runge-Kutta technique. Finding the profile of the electrode or pole piece of the electron optical device is the last step in the synthesis process. However, the form of the pole piece that generates the field distribution may be determined using the analytical solution of the paraxial-ray equation. as follows [17 and 18],

$$R_p(z) = 2 \sqrt{\frac{V(z) - V_p}{V(z)}} \quad (6)$$

Thus, in the case of a symmetrical charged particle lens, NI is equal to half of the lens excitation, and R_p is the radial height of the pole piece. V_p is the potential value at the pole piece surface. The magnetic scalar potential $V(z)$ has a second derivative, $V''(z)$, which may be calculated using eq. (1) as follows:

$$V''(z) = -(V_2 - V_1) \left(\frac{1.32z}{R} \right)^2 \tanh \left(\frac{1.32z}{R} \right) \text{sech}^2 \left(\frac{1.32z}{R} \right) \quad (7)$$

The radial and spiral distortion coefficients (D_r and D_s) are usually expressed by the following relations respectively [14]:

$$D_r = \left(\frac{\eta}{128V_r} \right) \int_{z_1}^{z_2} \left[\left(\frac{2\eta}{V_r} B_z^2 + 8B_z^2 \right) r_\alpha r_\gamma^3 - 4B_z^2 (r_\gamma^2 r_\alpha r_\gamma + r_\gamma^2 r_\alpha^2) \right] dz \quad (8)$$

$$D_s = \int_{z_1}^{z_2} \left[\frac{3}{128} \left(\frac{\eta}{V_r} \right)^{3/2} r_\alpha^2 B_z^3 + \frac{1}{16} \left(\frac{\eta}{V_r} \right)^{1/2} r_\alpha^2 B_z \right] dz \quad (9)$$

Where r_α and r_γ are the paraxial-ray equation's two linearly independent solutions eq. (4). The magnetic field's two terminal locations serve as the integration limits (z_1 and z_2). As mentioned above, the infinite magnification has been used to define the distortion coefficients throughout present work. Consequently, the values of these coefficients must computed referring the object position and hence such process required the definition of magnification. Therefore, magnification for the proposed imaging field calculated throughout by means of the following formula to this work [5];

$$M = \frac{L - (f_p)_{min}}{(f_p)_{min}} \quad (10)$$

Where $(fp)_{min}$ the minimum focal length of the imaging magnetic field and L , the distance between the magnetic lens and screen [21][22].

3. RESULTS AND DISCUSSION

Apart from the value of lens excitation, equation (1) shows only one optimization parameter namely the pole piece radius. In order to investigate the influence of this parameter on the optical properties of the proposed lens five values have been chosen namely (1, 2, 3, 4, and 5) in millimeter unit. However, V_1 and V_2 are kept fixed at the values -100 A-t and $V_2=100$ A-t (i.e. $NI=200$ A-t) respectively where the lens length (L) is assumed to be constant at the value 30 mm. Results have shown that the optimum imaging field belong to the value of $R= 1$ mm, see table-I.

Obviously, the increases in R -values leads to decreasing the maximum value of imaging field which in turn increasing its own half width. Actually, this is a reasonable result since increases of values of R results in increases the region of pole-face and hence reducing the magnetic flux density over there as long as NI maintained fixed. Indeed, such a result consist with the conventional one that may obtained in analysis procedure, see for example [8]. Consequently, the minimum projector focal length increases, and thereby lens magnification decreases, as long as R increased. However, it is important to mention that the first magnification point M_1 come to occurs at the same excitation parameter that is equal to 14.2 for all of the selected values of R . Furthermore, the lens excitation where the radial distortion vanished has a value about ~ 14.95 A-t and the corresponding values of spiral distortion for such an excitation are listed in table-I. Actually, this is an impressive result because it grant the proposed lens a wide range degree of freedom for usage. Strictly speaking, user has an opportunity to select the excitation parameter ~ 14.95 for operation instead of that of the first maximum magnification (i.e. 14.2) without a significant change in spiral distortion amount, and so the loss in magnification is less than $\sim 1\%$ [23][24].

Table 1: The proposed lens parameters and its corresponding focal properties for different values of pole piece radius at fixed values of excitation and lens length.

R (mm)	B_{max} (T)	W (mm)	$(fp)_{min}$ (mm)	$NI/Vr^{1/2}$	M	D_r (mm-1)	D_s (mm-1)	D_s (at $D_r=0$) (mm-1)
1	0.1659	1.3354	0.7576	14.2	38.6	0.311	1.970	2.203
2	0.0829	2.6708	1.515	14.2	18.8	0.078	0.492	0.521
3	0.0553	4.0063	2.273	14.2	12.2	0.035	0.220	0.242
4	0.0415	5.3417	3.031	14.2	08.9	0.019	0.123	0.113
5	0.0332	6.6771	3.788	14.2	06.9	0.123	0.079	0.081

Furthermore, table-I reveals that the magnification of the proposed lens get worse as the value of R increases. Although, this is a disadvantage remark that could be recorded against the lens under consideration, it can be ignored in comparison with enhancing of radial and spiral distortions. It is worth to mention that, such a reduction in the lens magnification can be compensate by adding another lens.

Figure-1 shows the magnetic scalar distribution along the specified region lens (i.e. 30 mm) for all of the selected values of R at the same excitation value $NI=200$ A-t. It is seen that, as the value of R increases the magnetic scalar potential spreads gradually along wide distances for the optical axes- z . This result can be thought as consequence for the constraints by means the scalar potential maintains fixed at the start/end lens. Accordingly, the corresponding distributions of the magnetic field are behaves as shown in figure-2. Indeed, the steadily extends of the scalar potential with fixed terminals value leads to make slope of these curves decreasing. Eventually, the magnetic flux density, that relates to scalar potential through relation (2), decreases in its amount and becomes much wider along the optical axes. Therefore, electrons interacts with magnetic field with deferent style as R increased. Strictly speaking, as R decreased these electrons interacts abruptly with magnetic field. In other word,

the time of interaction decreases as the magnetic field spread along the optical axes, however its axiom consequences [25][26].

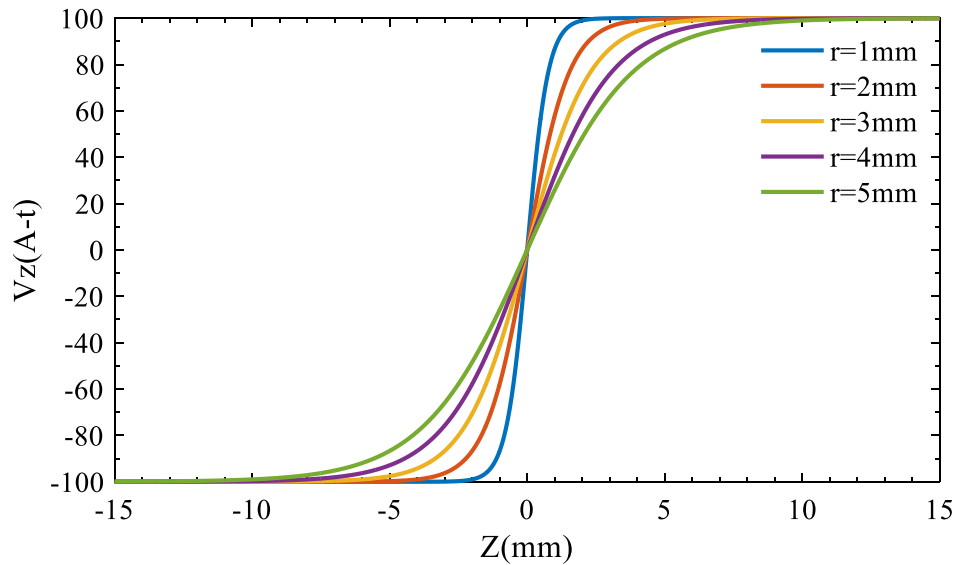


Figure-1: The axial magnetic scalar potential distributions for different values of the pole piece radius R.

Anyway, it is seam that, whenever an electrons beams take a long time to interact with imaging field, in sense of projector lens, the projector properties for such field being enhanced, see Table-I. Therefore, one may argued that, designer should keep in mind that it is preferable to design long projector lens rather a short one.

The reconstructed pole piece that belong to each value of R are plotted in figure-3. Obviously, the real bore get rise increase as the optimization parameter R increased and precisely the different between them are about 6%. Furthermore, the gab width also being wider as R increases indicating that the area where the magnetic field exist are increases. Due to that B_z values lowered and so extends along wide interval around the symmetry plane. Such a result, in fact, consistent with the inclusion mentioned in the last paragraph [27][28].

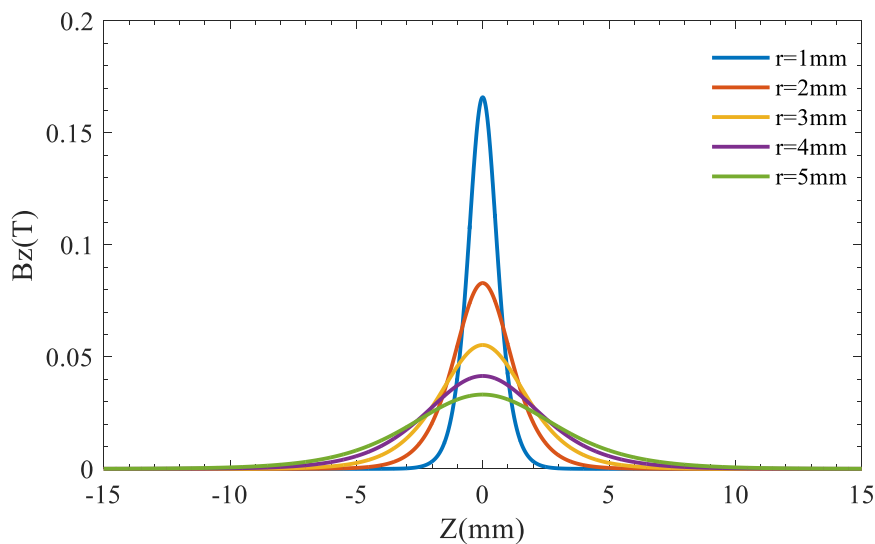


Figure-2: The axial magnetic field distributions for different values of the pole piece radius R.

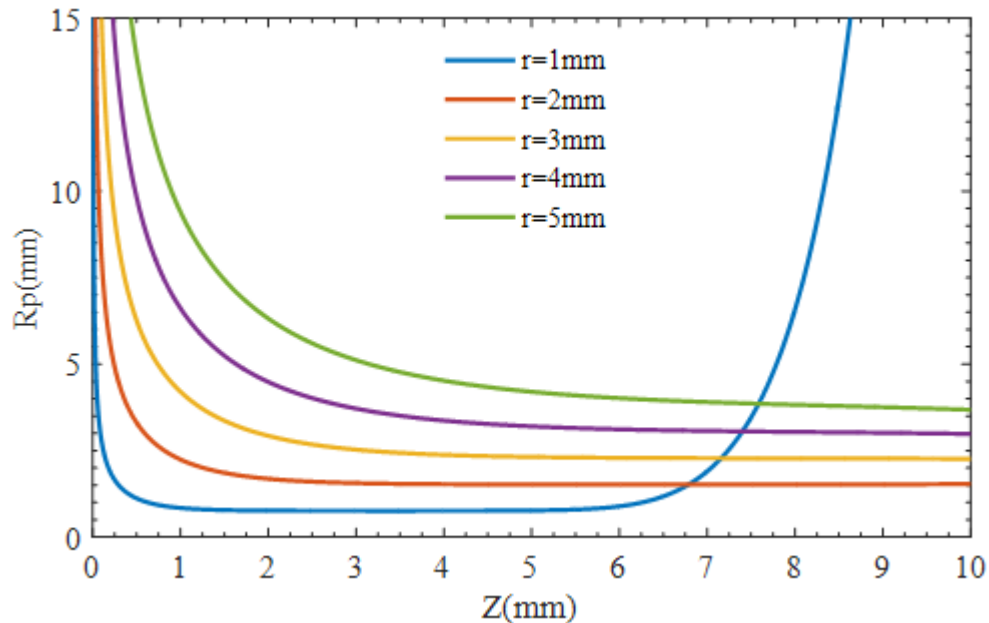


Figure-3: The reconstructed pole piece profile for different values of the pole piece radius R.

Figure-4 shows the behavior of the projector focal length for the proposed lens at various values for the optimization parameter R. Obviously, the intersection point between the electron beam and the optical axes-z gradually approach toward the lens center as the excitation parameter increases. The reason behind is the fixed value of excitation so the acceleration potential value should decrease to meet the increasing of the excitation parameter. Furthermore, the minimum value of each fp curve locate at an excitation parameter 14.2 referring to the first maximum magnification. Actually, an important inclusion may be recorded from behavior of fp curves in this figure that, there being a wide interval of $NI/\sqrt{V_r}$ where an approximately same magnification can obtain especially when R decreased. Therefore, manufacturing a long magnetic projector lens provides electron microscope users opportunities to adopt a wide range of $NI/\sqrt{V_r}$. Hence, users could espoused the one that matches with vanishing the radial distortion, or that have minimum value for the spiral distortion.

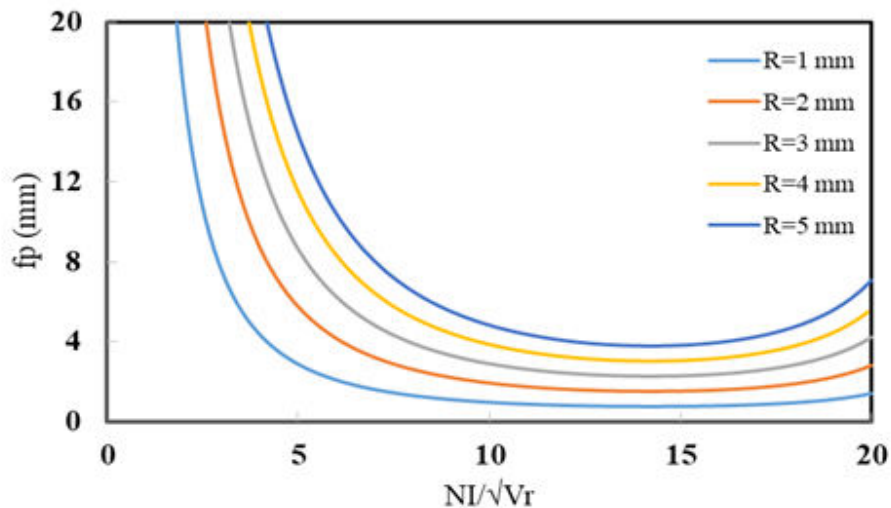


Figure-4: The projector focal length for different values of the pole piece radius R.

Variations of the radial distortion coefficient for the selected imaging fields are shown in figure-5. Results here emphasizes that the optical properties, specifically the radial distortion, gets significant enhancement whenever the values of the parameter R increases. However, it is seen that all of the D_r curves cross the zero at the excitation parameter ~ 14.95 A-t and hence such an excitation grand users an opportunity for operating the lens free from radial distortion. Furthermore, at this value of excitation parameter D_s has an insignificant amount relative to its value at first magnification point, as revealed by figure-6. Therefore, the designing of projector lenses with higher gap and/or bore width almost gives respectable values for distortions. Therefore, such a result gives indication for adopting either weak or long lens to be used in the imaging system of transmission electron microscope.

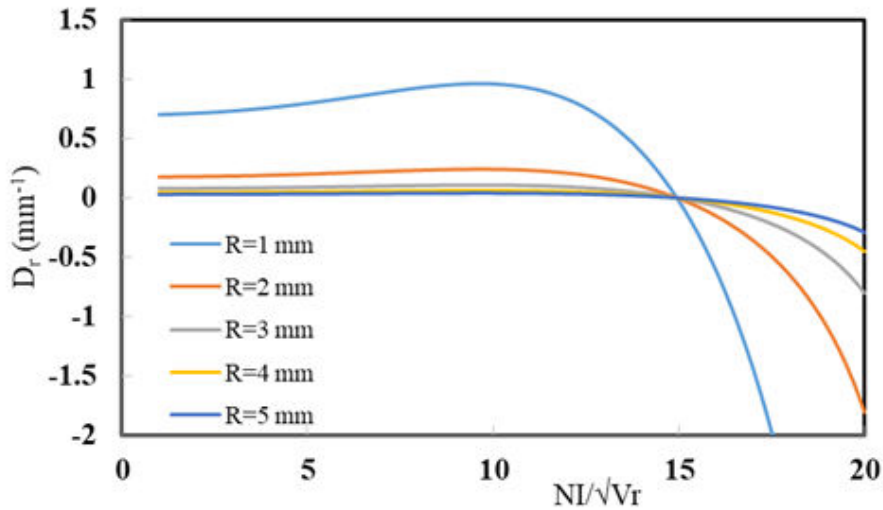


Figure-5: Variations of the radial distortion coefficient for different values of the pole piece radius R.

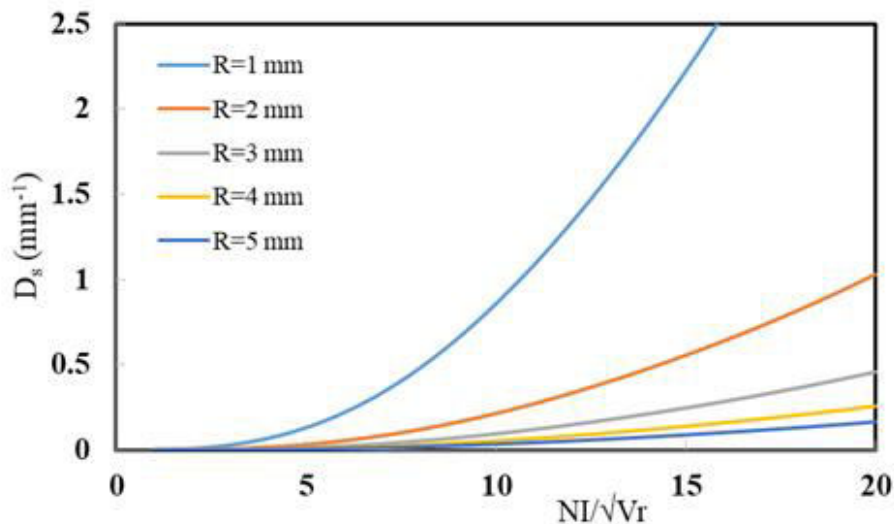


Figure-6: Variations of the spiral distortion coefficient for different values of the pole piece radius R.

Anyway, figure 7 summarize the outcome of the approach followed in the current work along with to find the excitation parameter that leads to get magnetic lens with free-radial distortion, low spiral distortion and the magnification that almost insignificantly differ from the magnification point.

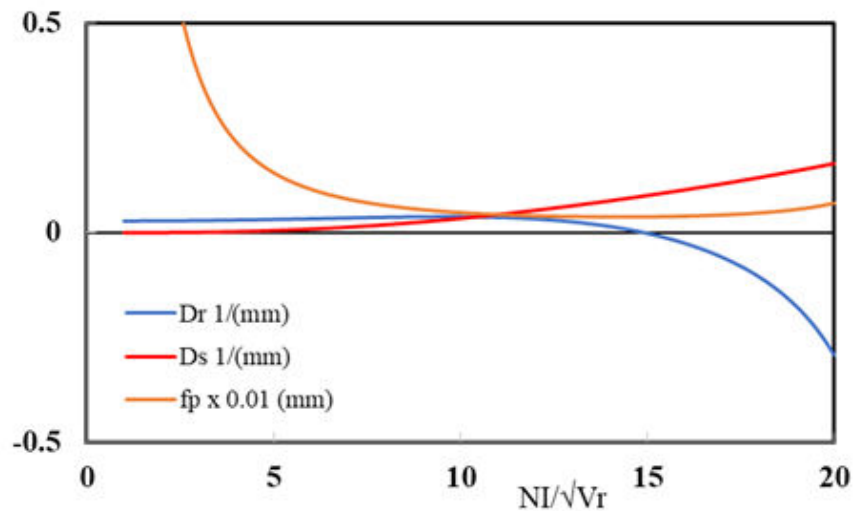


Figure-7: Variations of the spiral and radial distortion coefficients and the projector focal length for different values of the pole piece radius R.

5. CONCLUSIONS

According to the results of the presented approach several remarks could be recorded. Actually, one may advise designer to keep in mind that, the a projector lenses with higher gap and/or bore width almost gives respectable values of distortions. So, weak and long lens should a first choice in build up imaging system of transmission electron microscope. Furthermore, manufacturing a long magnetic projector lens provides electron microscope users opportunities to adopt a wide range of excitation parameter. Thereby, users could espoused the one that matches with vanishing the radial distortion, or that have minimum value for the spiral distortion.

REFERENCES

- [1] Yougui Liao *Practical, Electron Microscopy and Database*, An Online Book- www.globalsino.com/EM/, (2006),
- [2] Williams D. B. "*Transmission Electron Microscope*", Plenum Press. (2004),
- [3] Hillier, J., " *A Study of Distortion in Electron Microscope Projection Lenses* ". J. Appl. Phys. 17, 411-419, (1946)
- [4] Juma S. M and Mulvey T.. "*Electron Microscopy*". Vol. 1, ed. J. V. Sanders and D. J. Goodchild. (Australia Academy of sciences, Canberra). 134-135. (1974)
- [5] Juma S. M. and Mulvey T. "*Developments in Electron Microcopy and Analysis*", ed. J. A. Venables (London: Academic). 45- 48. (1976).
- [6] Juma S.M. and Mulvey T. (1978). "*Miniature Rotation- Free Magnetic Electron Lenses for the Electron Microscope*". J. Phys. E: Sci. Instrument 11, 759- 764.
- [7] Tsuno, K., Arai, Y., and Harada, Y., (1980). *Elimination of Spiral Distortion in Electron lenses by Means of Three-Ppolepiece Lens*. J. Elec. Micro. 1, 76-77.
- [8] Tsuno, K., and Harada Y., (1981). *Minimization of Radial and Spiral Distortion in Electron Microscopy through the Use of Triple Polepiece lens*. J. phys. 14, 313-319.
- [9] A.V. Crew, *On the peculiarities of monopole and multipole focusing*, Optik 112 (2001) 181–182.
- [10] A.S.A. Alamir, *Spiral distortion of magnetic lenses withfield of the form $B(z)azn$, $n = 1/4, 2, 3, 4$* , Optik 114 (2003) 525-528.

- [11] A.V. Grew, (2004), *Electron focusing in magnetic fields of the form Zn*, Optik 115, 31–35.
- [12] Mohammed J. Yaseen., *The Objective Properties of the Projector Magnetic Lenses*, IJETTCS (2013) **2**, 6 (54-59).
- [13] A. H. Al-Batat, M J Yaseen, S. R. Abbas, M. S. Al-Amshani and H S Hasan,(2018) “*Design of Magnetic Charged Particle Lens Using Analytical Potential Formula*”, IOP Conf. Series: Journal of Physics: Conf. Series, V(1003), Issue 012111.
- [14] El-Kareh A B and El-Kareh J C J (1970), *Electron beams, lenses, and optics* vol **2**, p**49**, (New York Academic)
- [15] Klempner O (1971), *Electron Optics* 3rd ed., (Cambridge)
- [16] Szilagyi M (1988), *Electron and ion optics*, Plenum Press New York and London
- [17] Szilagyi, M. 1985 Electron optical synthesis and optimization Proceeding of the IEEE, **73**, No. **3**
- [18] Al-Batat A. Hasan H. S., Ibrahim Husin H. M. and Yaseen M. J. (2016), Modulating Mathematical Function to be used in Electron Objective Lens , Journal of Advances in Physics Theories and Applications, vol 57, pp.8-15
- [19] Chaturvedi, Pooja, A. K. Daniel, and Vipul Narayan. "A Novel Heuristic for Maximizing Lifetime of Target Coverage in Wireless Sensor Networks." *Advanced Wireless Communication and Sensor Networks*. Chapman and Hall/CRC 227-242.
- [20] Chaturvedi, Pooja, Ajai Kumar Daniel, and Vipul Narayan. "Coverage Prediction for Target Coverage in WSN Using Machine Learning Approaches." (2021).
- [21] Kumar, Vaibhav, et al. "A Machine Learning Approach For Predicting Onset And Progression"“Towards Early Detection Of Chronic Diseases “." *Journal of Pharmaceutical Negative Results* (2022): 6195-6202.
- [22] Saxena, Aditya, et al. "Comparative Analysis Of AI Regression And Classification Models For Predicting House Damages In Nepal: Proposed Architectures And Techniques." *Journal of Pharmaceutical Negative Results* (2022): 6203-6215.
- [23] Narayan, Vipul, et al. "Severity of Lumpy Disease detection based on Deep Learning Technique." 2023 International Conference on Disruptive Technologies (ICDT). IEEE, 2023.
- [24] Mall, Pawan Kumar, et al. "A comprehensive review of deep neural networks for medical image processing: Recent developments and future opportunities." *Healthcare Analytics* (2023): 100216.
- [25] Mall, Pawan Kumar, et al. "Rank Based Two Stage Semi-Supervised Deep Learning Model for X-Ray Images Classification: AN APPROACH TOWARD TAGGING UNLABELED MEDICAL DATASET." *Journal of Scientific & Industrial Research (JSIR)* 82.08 (2023): 818-830.
- [26] Narayan, Vipul, et al. "A Comprehensive Review of Various Approach for Medical Image Segmentation and Disease Prediction." *Wireless Personal Communications* 132.3 (2023): 1819-1848.
- [27] Narayan, Vipul, et al. "7 Extracting business methodology: using artificial intelligence-based method." *Semantic Intelligent Computing and Applications* 16 (2023): 123.
- [28] kumar Mall, Pawan, et al. "Self-Attentive CNN+ BERT: An Approach for Analysis of Sentiment on Movie Reviews Using Word Embedding." *International Journal of Intelligent Systems and Applications in Engineering* 12.12s (2024): 612-623.